Journal of Solid Mechanics Vol. 2, No. 4 (2010) pp. 332-347

Elastic Buckling Analysis of Ring and Stringer-stiffened Cylindrical Shells under General Pressure and Axial Compression via the Ritz Method

A. Ghorbanpour Arani*, A. Loghman, A.A. Mosallaie Barzoki, R. Kolahchi

Department of Mechanical Engineering, Faculty of Engineering, University of Kashan, Kashan, Islamic Republic of Iran

Received 25 September 2010; accepted 11 November 2010

ABSTRACT

Elastic stability of ring and stringer-stiffened cylindrical shells under axial, internal and external pressures is studied using Ritz method. The stiffeners are rings, stringers and their different arrangements at the inner and outer surfaces of the shell. Critical buckling loads are obtained using Ritz method. It has been found that the cylindrical shells with outside rings are more stable than those with inside rings under axial compressive loading. The critical buckling load for inside rings is reducing by increasing the eccentricity of the rings, while for outside ring stiffeners the magnitude of eccentricity does not affect the critical buckling load. It has also been found that the shells with inside stringers are more stable than those with outside one. Moreover, the stability of cylindrical shells under internal and external pressures is almost the same for inside and outside arrangements of stringers. The results are verified by comparing with the results of Singer at the same loading and boundary conditions.

Keywords: Buckling analysis; Stiffened cylindrical shells; Ritz method.

1 INTRODUCTION

ELASTIC buckling analysis of stiffened cylindrical shells is more difficult than unstiffened one. The difficulty is more considerable when the shell is reinforced by irregular stiffeners with different material properties. Despite numerical analysis, it is not always possible to find out an exact solution. Although a stiffened shell may be modeled with an equivalent orthotropic shell, the results are only accurate if the stiffeners are distributed evenly and closely spaced.

One of the best methods for deriving eigen-values is the Ritz method. In this method, the assumed displacement functions may satisfy any combination of boundary conditions. The power of polynomial equations assumed for the displacement functions can be adjusted according to the boundary conditions in Ritz method. The general instability of a simply supported cylindrical shell under hydrostatic pressure is analyzed by Singer and Baruch [1]. They showed that the critical loads for inside-stiffened rings are about 10-15 percent greater than outside ones. Ghorbanpour et al. [2] studied elastic stability of cylindrical shell with an elastic core under axial compression by energy method. Their results show that using an elastic core increases elastic stability and significantly decreases the weight of the cylindrical shells. The stiffeners are attached to the shell as a fully welded ring. As Ojalvo and Newman [3] have pointed out, an effective line of attachment must be assumed in these cases. Thermoelastic buckling of thin cylindrical shell based on improved stability equations is analyzed by Eslami et al. [4].They showed the magnitude of thermoelastic buckling of thin cylindrical shells under different thermal loading and their results

* Corresponding author.
E-mail address: aghorban@kashanu.ac.ir; a_ghorbanpour@yahoo.com (A. Ghorbanpour Arani).

were extended to short and long thin cylindrical shells. Singer et al. [5] studied the effect of eccentricity on the critical buckling load of cylindrical shells under axial compression. Their results showed that the effect of eccentricity is very similar to clamped and simply supported shells. Buckling behavior of long steel cylindrical shells subjected to external pressure is studied by Hubner et al. [6]. Their numerical findings are verified by a set of experimental tests with a series of cylindrical shells subjected to external pressure. The tests provide the fundamental basis for the proposed improved assessment procedure for cylindrical shells. Buermann et al. [7] considered a semi- analytical model for local post-buckling analysis of stringer and frame-stiffened cylindrical panels. They captured the effects of local skin buckling and stiffener tripping. For the stiffeners, a uni- axial membrane stress state is assumed while plane stress state is considered for the skin. Strength and stability of double cylindrical shell structure subjected to hydrostatic external pressure is investigated by Din [8]. This research aims at the buckling of shell section with some curvature and cut out of a shell by two radial planes through the axis. Andrianov [9] proposed buckling analysis of discretely stringer-stiffened cylindrical shells. They show that a discrete character of reinforcement in the prebuckling state can be taken into account in an analytical way using the homogenisation approach.

This research aims at the buckling of stiffened cylindrical shells using Ritz method. The critical buckling load of stiffened cylindrical shells under different loading and stiffener arrangements are presented in this paper. The new specific work done in this paper is showing the significant effect of stringer and ring in inner and outer surface of cylindrical shell as reinforcer, loading condition include axial, lateral and hydrostatic pressure and eccentricity of reinforcer on the buckling load parameter λ of, for stiffened cylindrical shell.

2 DERIVATION OF THE ENERGY EQUATION

Consider a thin, isotropic, stiffened, cylindrical elastic shell with uniform thickness, radius, length, Young modulus, Poisson's ratio and shear modulus represented by *h, R, L, E,* ν and *G* respectively. The shell is reinforced by *N* number of rings and *M* number of stringers which may have different arrangements as shown in Fig. 1. The elastic strain energy for cylindrical shell due to planar stretching and bending of the shell in the coordinate systems is shown in Fig. 1 using Timoshenko relations and considering strain-displacement relations of Sanders theory yields [9].

$$
\begin{aligned}
U_{Shell} = \; & \frac{Eh}{2(1-\nu^2)}\int_0^L\int_0^{2\pi}\left[\left(\frac{\partial u}{\partial x}\right)^2+\frac{1}{R^2}\left(\frac{\partial v}{\partial \theta}-w\right)^2\right. \\
& \left.+\frac{2\nu}{R}\left(\frac{\partial v}{\partial x}\right)\left(\frac{\partial v}{\partial \theta}-w\right)+\frac{1-\nu}{2}\left(\frac{\partial v}{\partial x}+\frac{1}{R}\frac{\partial u}{\partial \theta}\right)^2\right] R\,d\theta\,dx \\
& +\frac{Eh^3}{24(1-\nu^2)}\int_0^L\int_0^{2\pi}\left[\left(\frac{\partial^2 w}{\partial x^2}\right)^2+\frac{1}{R^4}\left(\frac{\partial^2 w}{\partial \theta^2}+w\right)^2\right. \\
& \left.+\frac{2\nu}{R}\left(\frac{\partial^2 w}{\partial x^2}\right)\left(\frac{\partial^2 w}{\partial \theta^2}+w\right)+\frac{2(1-\nu)}{R^2}\left(\frac{\partial^2 w}{\partial x\partial \theta}+\frac{3}{4}\frac{\partial v}{\partial x}-\frac{1}{4R}\frac{\partial u}{\partial \theta}\right)^2\right] R\ \mathrm{d}\theta\ \mathrm{d}x
\end{aligned}
\tag{1}
$$

where u, v and w are the displacements in the longitudinal, tangential and radial directions, and x and θ are the longitudinal and circumferential coordinates, respectively. Only the strain energy due to the normal strain in the direction of the stiffeners axis and shear strain due to twisting about this axis are considered for the stiffeners Fig.1. The normal strain includes the effects of extension and bending of the stiffener about two axes. Thus - U_s, the total strain energy of the *s*th stringer- located at $\theta=\theta_s$, is [3].

$$
U_s=\frac{J_sG_s}{2}\int_0^L\left(\frac{1}{R}\frac{\partial^2 w}{\partial\theta\partial x}\right)^2_{\theta=\theta_s}\mathrm{d}x+\frac{E_s}{2}\int_0^L\left\{A_s\left[\frac{\partial u}{\partial x}+e_s\frac{\partial^2 w}{\partial x^2}-c_s\frac{\partial^2 v}{\partial x^2}\right]^2\right.
$$

$$+I_{zs}\left[\frac{\partial^2 v}{\partial x^2}+e_s\frac{1}{R}\frac{\partial^3 w}{\partial x^2\partial\theta}\right]^2+I_{yz}\left[\frac{\partial^2 w}{\partial x^2}+c_s\frac{1}{R}\frac{\partial^3 w}{\partial x^2\partial\theta}\right]^2$$
$$+2I_{yzs}\left[\frac{\partial^2 v}{\partial x^2}+e_s\frac{1}{R}\frac{\partial^3 w}{\partial x^2\partial\theta}\right]\times\left[\frac{\partial^2 w}{\partial x^2}+c_s\frac{1}{R}\frac{\partial^3 w}{\partial x^2\partial\theta}\right]\Bigg|_{\theta=\theta_s}\mathrm{d}x \tag{2}$$

where the sth stringer has an axial rigidity of E_sA_s, torsional rigidity of G_sJ_s, flexural rigidities about z and y axes of, E_sI_{zs} and E_sI_{ys}, respectively. I_{yz} is the product of inertia about y and z axes, e_s is the radial distance between the centroid of the cross-section of the sth stringer and its attachment line at mid-surface. While c_s is the circumferential distance between the centroid of the cross-sections of the sth and (s+1)th stringers. Note that a positive value of eccentricity e_s implies external stringer and a negative value of eccentricity represents an internal stringer.

Since the depth of the stiffener rings are much smaller than the shell radius, it is permissible to use Euler-Bernoulli theory for evaluating the strain-energy of the rings. Thus, strain energy of the kth ring is [3, 12]

$$U_k=\frac{1}{(R+e_k)^3}\Bigg[\frac{E_kI_{xk}}{2}\int_0^{2\pi}\left(w_k+\frac{\partial^2 w_k}{\partial\theta^2}\right)^2\mathrm{d}\theta$$
$$+\frac{E_kI_{zk}R^2}{2}\int_0^{2\pi}\left\{\left(\frac{\partial w_k}{\partial x}+\frac{1}{R}\frac{\partial^2 u_k}{\partial\theta^2}\right)+\frac{e_k}{R}\left(w_k+\frac{\partial^3 w_k}{\partial x\partial\theta^2}\right)\right\}^2\mathrm{d}\theta$$
$$+\frac{E_kA_k(R+e)^2}{2}\int_0^{2\pi}\left\{\left(\frac{\partial v_k}{\partial\theta}-w\right)+\frac{e_k}{R}\left(\frac{\partial v_k}{\partial\theta}+\frac{\partial^2 w_k}{\partial\theta^2}\right)\right\}^2\mathrm{d}\theta \tag{3}$$
$$+\frac{G_kJ_kR^2}{2}\int_0^{2\pi}\left(\frac{1}{R}\frac{\partial u_k}{\partial\theta}-\frac{\partial^2 w_k}{\partial x\partial\theta}\right)^2\mathrm{d}\theta\Bigg]$$

The kth ring-stiffener is located at L_k measured from the end of the shell with axial rigidity of E_kA_k, torsional rigidity of G_kJ_k, and flexural rigidities about z and x axis of E_kI_{zk} and E_kI_{xk}, respectively while e_k is the distance between the centroid of the kth ring-stiffener cross-section and shell mid-surface Fig.1. Like stringers a positive value of eccentricity e_k implies external ring while its negative value represents an internal one. The total potential energy of shell with a symmetric lateral pressure $q(x)$, and a uniform axial pressure p at its end, expressed as [13]:

$$V=-\int_0^L\int_0^{2\pi}\frac{q(x)}{2}\left\{\left[\frac{\partial^2 w}{\partial\theta^2}+w\right]w\right\}\mathrm{d}\theta\mathrm{d}x-\frac{\beta p}{4}\int_0^L\int_0^{2\pi}\left(\frac{\partial w}{\partial x}\right)^2R^2\mathrm{d}\theta\mathrm{d}x \tag{4}$$

where β is a scalar indicator which takes the value of 1 or 0, depending on whether there is or there is not an end axial pressure. In this analysis, the effect of shell imperfection in buckling is neglected when there is an end axial load. Thus, the total potential energy $\prod$ is given by:

$$\Pi=U_{Shell}+U_{Stringer}+U_{Ring}+V_{Loads}=U_{Shell}+\sum_{s=1}^{M}U_s+\sum_{k=1}^{N}U_k+V_{Loads}$$
$$=\frac{Eh}{2(1-\nu^2)}\int_0^L\int_0^{2\pi}\left[\left(\frac{\partial u}{\partial x}\right)^2+\frac{1}{R^2}\left(\frac{\partial v}{\partial\theta}-w\right)^2+\frac{2\nu}{R}\left(\frac{\partial v}{\partial x}\right)\left(\frac{\partial v}{\partial\theta}-w\right)+\frac{1-\nu}{2}\left(\frac{\partial v}{\partial x}+\frac{1}{R}\frac{\partial u}{\partial\theta}\right)^2\right]R\mathrm{d}\theta\mathrm{d}x$$
$$+\frac{Eh^3}{24(1-\nu^2)}\int_0^L\int_0^{2\pi}\left[\left(\frac{\partial^2 w}{\partial x^2}\right)^2+\frac{1}{R^4}\left(\frac{\partial^2 w}{\partial\theta^2}+w\right)^2\right.$$

$$
\begin{aligned}
&+\frac{2\nu}{R}\left(\frac{\partial^2 w}{\partial x^2}\right)\left(\frac{\partial^2 w}{\partial \theta^2}+w\right)+\frac{2(1-\nu)}{R^2}\left(\frac{\partial^2 w}{\partial x\partial \theta}+\frac{3}{4}\frac{\partial v}{\partial x}-\frac{1}{4R}\frac{\partial u}{\partial \theta}\right)^2\Bigg]R\mathrm{d}\theta\mathrm{d}x\\
&+\sum_{S=1}^{M}\Bigg\{\frac{J_s G_s}{2}\int_0^L\left(\frac{1}{R}\frac{\partial^2 w}{\partial\theta\partial x}\right)^2_{\theta=\theta_s}\mathrm{d}x+\frac{E_s}{2}\int_0^L\Bigg\{A_s\left[\frac{\partial u}{\partial x}+e_s\frac{\partial^2 w}{\partial x^2}-c_s\frac{\partial^2 v}{\partial x^2}\right]^2\\
&+I_{zs}\left[\frac{\partial^2 v}{\partial x^2}+e_s\frac{1}{R}\frac{\partial^3 w}{\partial x^2\partial\theta}\right]^2+I_{yz}\left[\frac{\partial^2 w}{\partial x^2}+c_s\frac{1}{R}\frac{\partial^3 w}{\partial x^2\partial\theta}\right]^2\\
&+2I_{yzs}\left[\frac{\partial^2 v}{\partial x^2}+e_s\frac{1}{R}\frac{\partial^3 w}{\partial x^2\partial\theta}\right]\times\left[\frac{\partial^2 w}{\partial x^2}+c_s\frac{1}{R}\frac{\partial^3 w}{\partial x^2\partial\theta}\right]\Bigg\}_{\theta=\theta_s}\mathrm{d}x\Bigg\}\\
&+\sum_{k=1}^{N}\Bigg\{\int_0^{2\pi}\Bigg\{\frac{E_k I_{zk}}{2}\frac{1}{R+e_k}\left(\frac{\partial w_k^r}{\partial x}+\frac{1}{R+e_k}\frac{\partial^2 u_k^r}{\partial\theta^2}\right)^2+\frac{E_k I_{xk}}{2}\frac{1}{(R+e_k)^3}\left(w_k^r+\frac{\partial^2 w_k^r}{\partial\theta^2}\right)\\
&+\frac{E_k A_k}{2}\frac{1}{R+e_k}\left(\frac{\partial v_k^r}{\partial\theta}-w_k^r\right)^2+\frac{G_k J_k}{2}\frac{1}{R+e_k}\left(-\frac{\partial^2 w_k^r}{\partial x\partial\theta}+\frac{1}{R+e_k}\frac{\partial u_k^r}{\partial\theta}\right)^2\Bigg\}\mathrm{d}\theta\Bigg\}\\
&-\int_0^L\int_0^{2\pi}\frac{q(x)}{2}\left\{\left[\frac{\partial^2 w}{\partial\theta^2}+w\right]w\right\}\mathrm{d}\theta\mathrm{d}x\;-\;\frac{\beta p}{4}\int_0^L\int_0^{2\pi}\left(\frac{\partial w}{\partial x}\right)^2 R^2\mathrm{d}\theta\mathrm{d}x
\end{aligned}
\tag{5}
$$

In this work, only one term of the double Fourier series is taken into account. It is noted that one term has a good accuracy. For computational simplicity and accuracy of the total potential energy, variables x and θ can be separated using the following trigonometric functions.

$$u=u(x,\theta)=u(x)\sin n\theta \tag{6a}$$

$$v=v(x,n)=v(x)\cos n\theta \tag{6b}$$

$$w=w(x,\theta)=w(x)\sin n\theta \tag{6c}$$

where n is the circumferential wave number. For generality and convenience, also, the following non-dimensional terms are considered:

$$
\begin{aligned}
&\overline{w}=\frac{w}{R},\quad \overline{u}=\frac{u}{h},\quad \overline{v}=\frac{v}{h},\quad \overline{x}=\frac{x}{L}\\
&\overline{J}_k=\frac{J_k}{Rh^3},\quad \overline{e}_s=\frac{e_s}{h},\quad \overline{C}_s=\frac{c_s}{h},\quad \overline{E}_s=\frac{E_s}{E},\quad \overline{I}_{zs}=\frac{I_{zs}}{Rh^3}\\
&\overline{E}_k=\frac{E_k}{E},\quad \overline{e}_k=\frac{e_k}{h},\quad \overline{I}_{zk}=\frac{I_{zk}}{Rh^3},\quad \overline{I}_{xk}=\frac{I_{xk}}{Rh^3},\quad \overline{A}_k=\frac{A_k}{h^2}\\
&\overline{I}_{ys}=\frac{I_{ys}}{Rh^3},\quad \overline{I}_{yzs}=\frac{I_{yzs}}{Rh^3},\quad \overline{A}_s=\frac{A_s}{h^2},\quad \overline{J}_s=\frac{J_s}{Rh^3}\\
&\alpha=\frac{R}{L},\quad \xi=\frac{h}{R},\quad \psi(\overline{x})=\frac{q(x)}{pL},\quad \lambda=\frac{pR(1-\nu^2)}{Eh}
\end{aligned}
\tag{7}
$$

By substituting Eqs. (6a), (6b), (6c) and (7) into Eq. (5) and integration with respect to θ, the non-dimensional total potential energy function $\overline{\Pi}$ may be expressed as:

$$\overline{\Pi}=\frac{2\pi(1-\nu^2)}{\pi RLEh}=\overline{U}_c+\sum_{s=1}^{M}\overline{U}_s+\sum_{k=1}^{N}\overline{U}_k+\overline{V} \tag{8}$$

The non-dimensional strain energy function of cylindrical shell is:

$$\overline{U}_c = \int_0^1 \left\{ \alpha^2\xi^2\left(\frac{\mathrm{d}\overline{u}}{\mathrm{d}\overline{x}}\right)^2 + (\xi n\overline{v}+\overline{w})^2 - 2\nu\alpha\xi\left(\frac{\mathrm{d}\overline{u}}{\mathrm{d}\overline{x}}\right)(\xi n\overline{v}+\overline{w}) \right.$$
$$+\frac{1\text{-}\nu}{2}\xi^2\left(\alpha\frac{\mathrm{d}\overline{v}}{\mathrm{d}\overline{x}}+n\overline{u}\right)^2 + \frac{\xi^2}{12}\left[\alpha^4\left(\frac{\mathrm{d}^2\overline{w}}{\mathrm{d}\overline{x}^2}\right)^2 + \overline{w}^2(1-n^2)^2\right. \tag{9}$$
$$\left.\left. +2\nu\alpha^2\left(\frac{d^2\overline{w}}{d\overline{x}^2}\right)\overline{w}(1-n^2) + 2(1-\nu)\alpha^2\left(n\frac{d\overline{w}}{d\overline{x}}+\frac{3}{4}\xi\frac{d\overline{v}}{d\overline{x}}-\frac{1}{4}\frac{n\xi}{\alpha}\overline{u}\right)^2\right]\right\}\mathrm{d}\overline{x}$$

and the non-dimensional strain energy function of stringers-stiffened:

$$\sum_{s=1}^{M}\overline{U}_s = \sum_{s=1}^{M}\left\{\frac{(1-\nu^2)}{\pi}\bar{E}_s\left[\bar{U}_{s1}+\bar{U}_{s2}+\bar{U}_{s3}+\bar{U}_{s4}+\bar{U}_{s5}\right]\right\} \tag{10}$$

where

$$\bar{U}_{s1} = \frac{\bar{J}_s\alpha^2\xi^2n^2}{2(1+\nu)}\cos^2 n\theta\int_0^1\left(\frac{\mathrm{d}\overline{w}}{\mathrm{d}\overline{x}}\right)^2\mathrm{d}\overline{x} \tag{11a}$$

$$\bar{U}_{s2} = \overline{A}_s\xi\alpha^2\left\{\xi^2\sin^2 n\theta\int_0^1\left(\frac{\mathrm{d}\overline{u}}{\mathrm{d}\overline{x}}\right)^2\mathrm{d}\overline{x} + \overline{e}_s^{\,2}h^2\sin^2 n\theta\int_0^1\left(\frac{\mathrm{d}^2\overline{w}}{\mathrm{d}\overline{x}^2}\right)^2\mathrm{d}\overline{x}\right.$$
$$+2\overline{e}_s h\xi\sin^2 n\theta\int_0^1\left(\frac{\mathrm{d}\overline{u}}{\mathrm{d}\overline{x}}\right)\left(\frac{\mathrm{d}^2\overline{w}}{\mathrm{d}\overline{x}^2}\right)\mathrm{d}\overline{x} + \overline{c}_s^{\,2}h^2\alpha^2\xi^2\cos^2 n\theta\int_0^1\left(\frac{\mathrm{d}^2\overline{v}}{\mathrm{d}\overline{x}^2}\right)^2\mathrm{d}\overline{x}$$
$$\left.\text{-2 }\sin n\theta\,\cos n\theta\left[\overline{c}_s h\alpha^2\xi^2\int_0^1\left(\frac{\mathrm{d}\overline{u}}{\mathrm{d}\overline{x}}\right)\left(\frac{\mathrm{d}^2\overline{v}}{\mathrm{d}\overline{x}^2}\right)\mathrm{d}\overline{x} + \overline{e}_s\overline{c}_s h^2\alpha^2\xi\int_0^1\left(\frac{\mathrm{d}^2\overline{w}}{\mathrm{d}\overline{x}^2}\right)\left(\frac{\mathrm{d}^2\overline{v}}{\mathrm{d}\overline{x}^2}\right)\mathrm{d}\overline{x}\right]\right\} \tag{11b}$$

$$\bar{U}_{s3} = \bar{I}_{zs}h^2\alpha^2\xi^2\cos^2 n\theta\left[\int_0^1\left(\frac{\mathrm{d}^2\overline{v}}{\mathrm{d}\overline{x}^2}\right)^2\mathrm{d}\overline{x} + \overline{e}_s^{\,2}n^2\int_0^1\left(\frac{\mathrm{d}^2\overline{w}}{\mathrm{d}\overline{x}^2}\right)^2\mathrm{d}\overline{x} + 2\overline{e}_s n\int_0^1\left(\frac{\mathrm{d}^2\overline{v}}{\mathrm{d}\overline{x}^2}\right)\left(\frac{\mathrm{d}^2\overline{w}}{\mathrm{d}\overline{x}^2}\right)\mathrm{d}\overline{x}\right] \tag{11c}$$

$$\bar{U}_{s4} = \bar{I}_{ys}h^2\alpha^2\left[\sin n\theta + \overline{c}_s n\xi\cos n\theta\right]^2\int_0^1\left(\frac{\mathrm{d}^2\overline{w}}{\mathrm{d}\overline{x}^2}\right)^2\mathrm{d}\overline{x} \tag{11d}$$

$$\bar{U}_{s5} = 2\bar{I}_{yzs}h^2\alpha^2\xi\cos n\theta\,(\sin n\theta + \overline{c}_s n\xi\cos n\theta)\left[\int_0^1\left(\frac{\mathrm{d}^2\overline{v}}{\mathrm{d}\overline{x}^2}\right)\left(\frac{\mathrm{d}^2\overline{w}}{\mathrm{d}\overline{x}^2}\right)\mathrm{d}\overline{x} + \overline{e}_s n\int_0^1\left(\frac{\mathrm{d}^2\overline{w}}{\mathrm{d}\overline{x}^2}\right)^2\mathrm{d}\overline{x}\right] \tag{11e}$$

The non-dimensional strain energy functional of ring-stiffened is:

$$\sum_{k=1}^{N}\overline{U}_k = \frac{1\text{-}\nu^2}{(1+\xi\overline{e}_k)^3}\bar{E}_k\alpha\xi^2\left[\bar{U}_{k1}+\bar{U}_{k2}+\bar{U}_{k3}+\bar{U}_{k4}\right] \tag{12}$$

where

$$\bar{U}_{k1} = \overline{I}_{zk}\left[\alpha(1+\xi\overline{e}_k - n^2\xi\overline{e}_k)\frac{\mathrm{d}\overline{w}_k}{\mathrm{d}\overline{x}} - \xi n^2\overline{u}_k\right]^2 \tag{13a}$$

$$\bar{U}_{k2} = \overline{I}_{xk}\left[(1_k - n^2)\overline{w}_k\right]^2 \tag{13b}$$

$$\bar{U}_{k3} = \overline{\mathrm{A}}_{\mathrm{k}}\frac{(1+\xi\overline{e}_k)^2}{\xi}\left[\xi n(1+\xi\overline{e}_k)\overline{v}_k + (1+n^2\xi\overline{e}_k)\overline{w}_k\right]^2 \tag{13c}$$

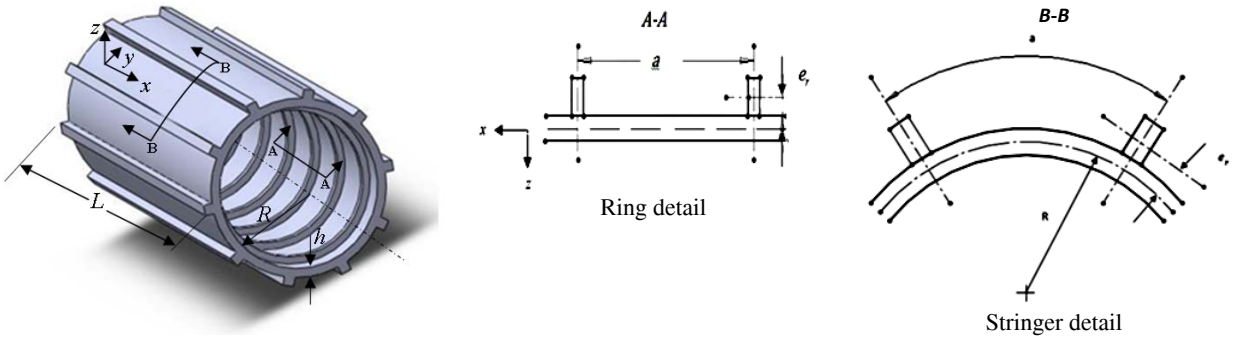

Fig. 1
Geometry and coordinate system of a stiffened cylindrical shell.

$$\bar{U}_{k4} = \frac{\bar{\mathrm{J}}_{\mathrm{k}}}{2(1+\nu_{\mathrm{k}})}\left[-\xi n\bar{u}_k + \alpha n\frac{\mathrm{d}\bar{w}_k}{\mathrm{d}\bar{x}}\right]^2 \tag{13d}$$

The non-dimensional potential energy function with axial and lateral pressure is written as:

$$\bar{V} = \bar{V}_l + \bar{V}_a = -\lambda\int_0^1\left[\psi(\bar{x})\bar{w}^2(1-n^2) + \frac{\beta\alpha^2}{2}\left(\frac{\mathrm{d}\bar{w}}{\mathrm{d}\bar{x}}\right)^2\right]\mathrm{d}\bar{x} \tag{14}$$

where $\bar{V}_l$ and $\bar{V}_a$ are the non-dimensional potential energy of the lateral and the axial pressures, respectively.

3 DERIVING EIGEN-VALUE EQUATION

In continuous members like cylindrical shells, infinite coordinates are needed to investigate the stability of the deformed shape. The critical load is determined by using polynomial function of the Ritz method .This method have a good agreement with the critical load which is determined in the previous studies. The polynomial functions in Ritz method must satisfy all kinematic boundary conditions. In simply supported condition $(w_{,xx} = w = v = 0)$, moreover, the following Ritz functions for cylindrical shells may be adopted as [11]:

$$\bar{u} = \left[\sum_{i=1}^{m} c_i\bar{x}^{i-1}\right] = \sum_{i=1}^{m} c_i\bar{u}_i \tag{15a}$$

$$\bar{v} = \left[\sum_{i=1}^{m} d_i\bar{x}^{i-1}\right][\bar{x}][1-\bar{x}] = \sum_{i=1}^{m} d_i\bar{v}_i \tag{15b}$$

$$\bar{w} = \left[\sum_{i=1}^{m} e_i\bar{x}^{i-1}\right][\bar{x}][1-\bar{x}] = \sum_{i=1}^{m} e_i\bar{w}_i \tag{15c}$$

where m is the number of polynomial terms of displacement function. Applying the Ritz method on the non-dimensional total potential energy function leads to:

$$\frac{\partial\bar{\Pi}}{\partial c_i} = 0 \qquad i = 1,2,...,m \tag{16a}$$

$$\frac{\partial\bar{\Pi}}{\partial d_i} = 0 \qquad i = 1,2,...,m \tag{16b}$$

$$\frac{\partial \bar{\Pi}}{\partial e_i} = 0 \qquad i = 1,2,...,m \tag{16c}$$

Substituting displacements of Eqs. (15a), (15b) and (15c) in Eq.(8) and then in Eqs.(16a), (16b) and (16c) yields:

$$([K] - \lambda [G])\{C\} = \{0\} \tag{17}$$

where

$$\{C\} = \begin{Bmatrix} \{c\} \\ \{d\} \\ \{e\} \end{Bmatrix}, \quad \{c\} = \begin{Bmatrix} c_1 \\ c_2 \\ \vdots \\ c_n \end{Bmatrix}, \quad \{d\} = \begin{Bmatrix} d_1 \\ d_2 \\ \vdots \\ d_n \end{Bmatrix}, \quad \{e\} = \begin{Bmatrix} e_1 \\ e_2 \\ \vdots \\ e_n \end{Bmatrix} \tag{18}$$

And the elements of the stiffness matrix are:

$$[K] = [K]^c + \sum_{s=1}^{M} [K]^s + \sum_{k=1}^{N} [K]^k \tag{19}$$

The elements of stiffness $[K]$ and geometric stiffness $[G]$ matrices are given in Appendix A. To determine the buckling load parameter λ, which is defined in non-dimensional form as $\lambda = P_r \backslash (1-\nu^2)/(Eh)$, it is necessary to obtain the nontrivial solution of Eq. (17). Therefore, the determinant of the coefficient matrix in Eq. (17) is set equal to zero. By solving the linear eigenvalue problem the smallest eigenvalue which is minimum buckling load parameter $(\lambda_{\min})$ and the corresponding eigen-vector $\{C\}$, can be found. It is noted that the buckling load is computed by multiplying the initial load with this smallest eigenvalue. The important point in solution of the eigen-value equation for obtaining minimum buckling critical load is selection of appropriate values for *m* and *n* parameters. Appropriate value for *n* may be chosen by trial which leads to the smallest eigen-value λ_{cr}.

4 NUMERICAL RESULTS AND DISCUSSION

The numerical results of the critical buckling load of stiffened cylindrical shells under different loading, boundary conditions and stiffener arrangements are presented in this paper. These arrangements included inner and outer rings and stringers stiffener with variable distances. The results were considered for boundary conditions of free and fixed ends and loading conditions of axial, lateral and hydrostatic pressure or combinations of them. The results obtained by solving the eigen-value equation of Ritz method are in good agreement with those reported by other researchers.

4.1 Stiffened cylindrical shell with rings under axial pressure

The influence of the ring-stiffened shell geometry on axial pressure buckling parameter $\Lambda = PR/\pi D$, are shown for both inside and outside rings in Figs. 2 and 3 respectively. The numerical results of the buckling parameter are then compared with those obtained from Singer et al. [5] in Table 1 which indicate that cylindrical shells with outside rings have more stability than those with inside rings under axial pressure. The numerical results are in good agreement with those reported by Singer et al. [5]. The eccentricity effect for cylindrical shell with stiffened rings under axial pressure on buckling load parameter λ is shown in Fig. 2. With inside rings, in general, the buckling load is reduced by decreasing the eccentricity of the rings, whereas with outside rings the magnitude of the eccentricity does not affect the buckling load. The curves of buckling load parameter variation in cylindrical shell with 40 evenly spaced external ring-stiffeners under axial, lateral and hydrostatic pressures verses length variations are drawn in Fig. 3. These curves show that for small ratio of *R*/*L*, there is little difference between the values of shell buckling load parameter under hydrostatic and lateral pressures, but as *R*/*L* increases, this difference increases

too, and the stability of ring-stiffened cylindrical shell under axial compression becomes greater than hydrostatic and lateral pressures.

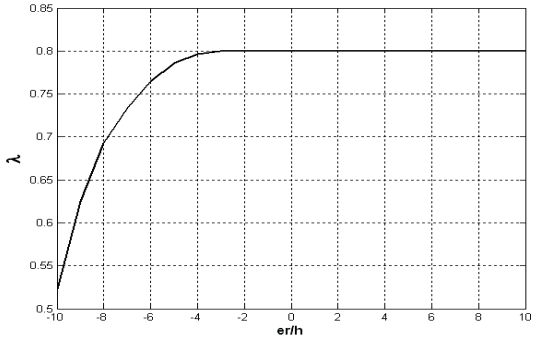

Fig. 2
Eccentricity effect on axial pressure buckling parameter λ, for ring stiffened cylindrical shell.

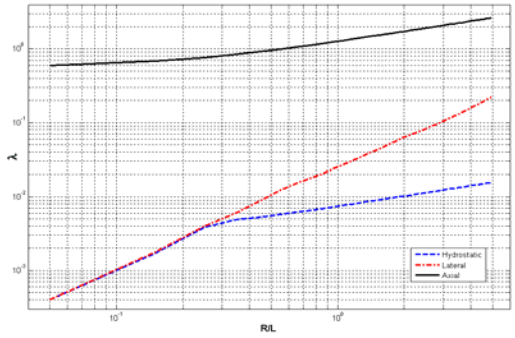

Fig. 3
Comparison of the buckling load parameter λ, for ring stiffened cylindrical shell under hydrostatic, lateral and axial pressures.

Table 1
Comparison studies of the buckling axial pressure parameter Λ, for ring stiffened cylindrical shell ($L/R=0.5,\ \nu=0.3$)

				Present study				Singer,Baruch,Harari[5]			
R/h	A_r/bh	I/bh^3		Outside(+)		Inside(-)		Outside(+)		Inside(-)	
$\lvert e_r/h\rvert$				A^+	n	A^-	n	A^+	n	A^-	n
50	0.5	5	5	834.5	0 *	501.4	4	809.4	0*	718.4	3
100				1632.6	0	846.4	6	1619	0	1420	4
250				4048.5	0	2107.1	10	4048	0	3578	6
500				8102.7	0	4264.5	14	8094	0	7063	8
1000				16194.0	0	8428.5	20	16190	0	14050	11
2000				32411.0	0	16781.0	28	32380	0	28080	16
250	0.5	2	0	4015.7	5	**		4016	5	**	
		5		4032.8	3			4033	3		
		20		4044.2	2			4044	2		
		40		4046.4	1			4046	1		
		200		4048.5	0			4048	0		
250	0.5	5	0.5	4048.4	1	3993.4	4	4048	0	3994	4
		2	1	4048.5	0	3813.2	8	4048	0	3854	7
		40	1	4048.5	0	4029.4	2	4048	0	4030	2

*n=0 means axisymmetric buckling.
**Results for outside and inside rings are the same because of e_r=0.

4.2 Stiffened cylindrical shell with stringers under axial pressure

The influence of the stringer-stiffened shell geometry on axial pressure buckling parameter $\Lambda = PR/\pi D$ is shown in Figs. 4 and 5. To evaluate the accuracy of the Ritz method in this study, these results are compared in Table2 with those obtained by Singer et al. [5]. The buckling load parameter for stiffened cylindrical shell with 60 stringers located either inside or outside, under axial load, is shown in Fig. 4. The curves of buckling load parameter are also plotted in this figure to indicate the influence of the stringers on the buckling load in order to compare with the case of an unstiffened equivalently thickened cylinder. It is noted that the buckling load diagram of the unstiffened shell is dependent on the non-dimensional parameter *R*/*L*, but variation of this case become low compared with other cases. This shows the shell length variation more specifically. This point was also demonstrated for buckled shells under axial compression in Timoshenko relation [6]:

$$\sigma_{cr} = \frac{N_{cr}}{h} = \frac{Eh}{R\sqrt{3(1-\nu^2)}} \tag{20}$$

However, the difference between the critical axial load for inside and outside stringers decreases with increase in the shell length. The difference between two curves increases with increase in *R*/*L*, and buckling load parameter for shells with outside stringer is more than those with inside ones. In contrary, the shells with inside stringers are more stable than those with outside ones for high ratio of *R*/*L*, i.e. shell with short lengths. The effect of rings and stringers on buckling load parameter for shells under axial pressure is compared in Fig. 5 which data points associated to this figure has been shown in Table 3. These curves and table indicate that under axial load, outside rings have more stability than inside ones. It can also be seen that for low *R*/*L* ratios, there is no significant variations for both rings and stringers. For *R*/*L* ratios of higher than 0.2, the stability of the stringers improves considerably compared with that of the rings, as λ increases rapidly. It is observed from Table 3 that buckling load parameter, λ, in case of equivalent shell is validated by ref [4].

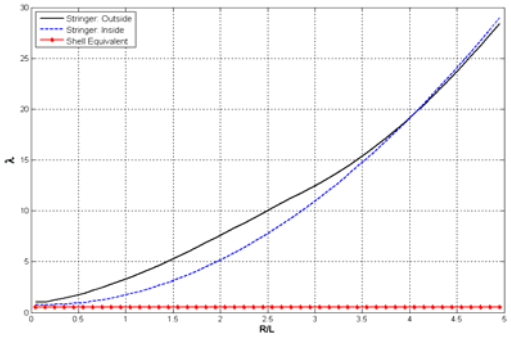

Fig. 4
Axial pressure buckling parameter λ, for stringer stiffened cylindrical shell.

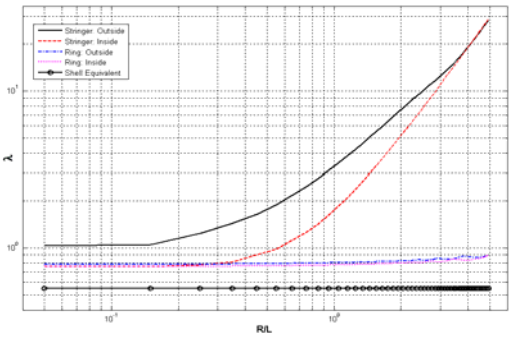

Fig. 5
Comparison of ring and stringer effects on buckling load parameter λ, for stiffened cylindrical shell under axial pressure.

Table 2
Effect of geometry parameters on the axial pressure buckling parameter Λ , for stringer stiffened cylindrical shell

L/R	R/h	A_s/bh	I_{zz}/bh^3	Present study				Singer et al. [5]			
				Outside(+)		Inside(-)		Outside(+)		Inside(-)	
$\lvert e_s/h \rvert$				A^+	n	A^-	n	A^+	n	A^-	n
1.0	250	1.5	5	24376	10	8432.4	7	23380	10	8432	7
7											
	500			33897	13	10148	10	33900	13	10150	10
	1000			50062	15	15176	13	50060	15	15180	13
1.0	250	1.5	5	39707	10	14781	7	39700	10	14780	7
10											
	500			51722	13	15731	9	51720	13	15730	9
	1000			70695	16	19243	12	70690	16	19240	12
2.0	500	1.5	5	25888	9	7471.3	8	25890	9	7471	8
10											
		3.0		39654	10	7596.6	7	39650	10	7597	7
		5.0		54734	10	7635.7	7	81770	12	13970	10

Table 3
Effect of rings and stringers on buckling load parameter versus *R/L* for shells under axial pressure (Data point associated to Fig. 5)

Stiffeners Log (R/L)	Shell Equivalent (Ref. [4])	Ring:Inside	Ring:Outside	Stringer:Inside	Stringer:Outside
0.10	0.2418	0.6212	0.6321	0.6214	1.0020
0.40	0.2428	0.6222	0.6332	0.8226	1.0402
0.70	0.2444	0.6254	0.6354	1.0242	1.1412
1.00	0.2510	0.6318	0.6434	1.1824	1.2412
1.30	0.2555	0.6328	0.6464	10.044	10.046

4.3 Stiffened cylindrical shell with stringers under lateral pressure and hydrostatic pressure

In this section the influence of stringers on buckling load parameter under lateral and hydrostatic pressures is investigated. For better understanding, stringers and rings are compared and shown in separate curves. The geometrical dimensions of the proposed stiffeners and shell are as follow:

$$L/R = 3.98, \quad R/H = 338, \quad I/bh^3 = 1.03, \quad A/bh = 9.79, \quad e/h = 5.83$$

The influence of rings and stringers on buckling load parameter under lateral pressure and hydrostatic pressure are shown in Figs. 6 and 7, respectively. The curve of unstiffened equivalent thickened shell is also plotted in these figures. As shown in Figs. 6 and 7, the stability of stiffened cylindrical shell by ring under lateral or hydrostatic pressures is more than the one stiffened by stringers. Buckling load of shell with inside and outside rings are almost the same, thus short shell length does not change the value of buckling load of rings stiffened shells under hydrostatic pressure. Similar to the curves shown in Figs. 6 and 7, stiffened shells with outside stringers under lateral and hydrostatic pressures are more stable than those with inside stringers. The stability of unstiffened long shells is more than stringer-stiffened shells. The buckling load parameter of stringer-stiffened cylindrical shell under hydrostatic, lateral and axial pressures is compared in Fig. 8. As shown in Fig. 8, the stability of stringers against axial loads are much more than lateral and hydrostatic pressures, and the stability of stringer stiffened cylindrical shell against lateral and hydrostatic loads are the same, and with increase in *R/L*, this stability increases too in the same manner.

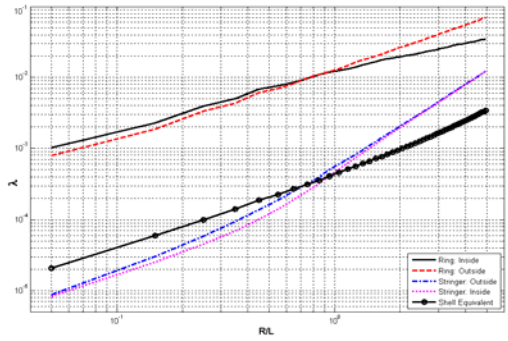

Fig. 6
Comparison of ring and stringers effect on buckling load parameter λ, for stiffened cylindrical shell under lateral pressure.

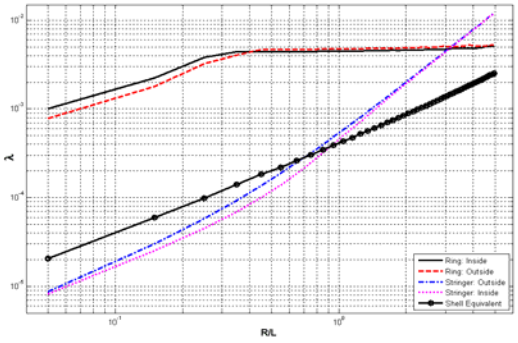

Fig. 7
Comparison of ring and stringers effect on buckling load parameter λ, for stiffened cylindrical shell under hydrostatic pressure.

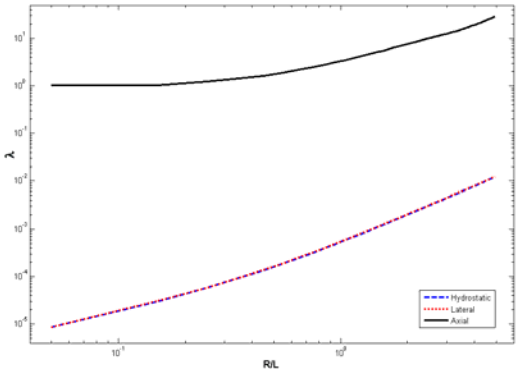

Fig. 8
Comparison of the buckling load parameter λ, for stringer stiffened cylindrical shell under hydrostatic, lateral and axial pressures.

4.4 Stiffened cylindrical shell with combination of stringers and rings

In this section, the influence of stringers and rings combination on buckling load parameter are investigated. A simply supported cylindrical shell with 60 stringers and 40 evenly spaced rings with the following dimensions are analyzed here:

$$L/R = 3.98, \quad R/H = 338, \quad I/bh^3 = 1.03, \quad A/bh = 9.79, \quad e/h = 5.83$$

In Figs. 9-14, variation of buckling load versus *R/L* under axial, lateral and hydrostatic pressure is shown. Fig. 9 illustrates the best stability position of stiffened shell under axial pressure when stringers and rings are outside the shell surface. However Fig. 10 shows that for very small values of *R/L*, and very long stiffened cylinder shells under axial pressure, outside stringers and inside rings represent maximum stability. The critical buckling load parameter of stiffened cylindrical shell, under lateral and axial pressures, for small *R/L* (Figs. 12 and 14) have very little

difference (about 10^{-5}). This shows that stability behavior of long shell under lateral and hydrostatic pressures are very similar. The number of circumferential waves is also the same during buckling. In stiffened shell under lateral and hydrostatic pressure, with high *R/L* ratio (Figs. 11 and 13), the shell stability is more when rings and stringers are outside the cylindrical shell.

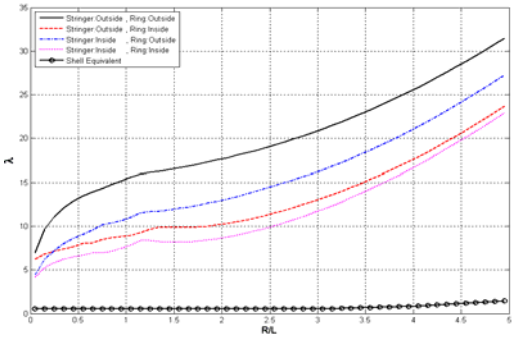

Fig. 9
Axial pressure buckling parameter λ, for stringers and rings stiffened cylindrical shell ($R / L\langle 5$).

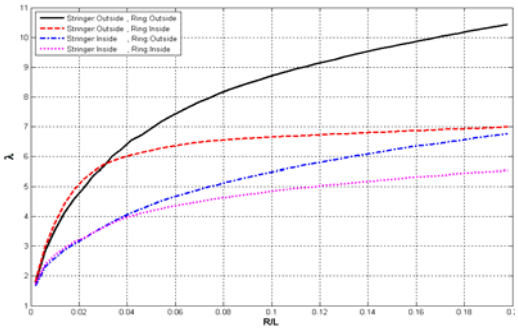

Fig. 10
Axial pressure buckling parameter λ, for stringers and rings stiffened cylindrical shell ($R / L\langle 0.2$).

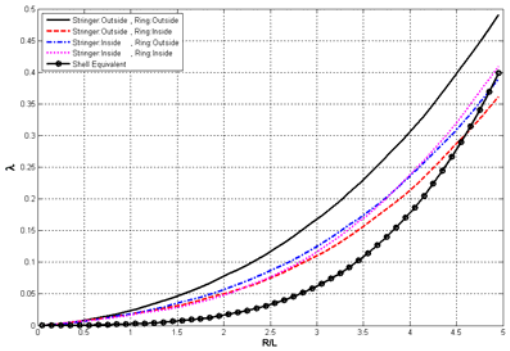

Fig. 11
Lateral pressure buckling parameter λ, for stringers and rings stiffened cylindrical shell ($R / L\langle 5$).

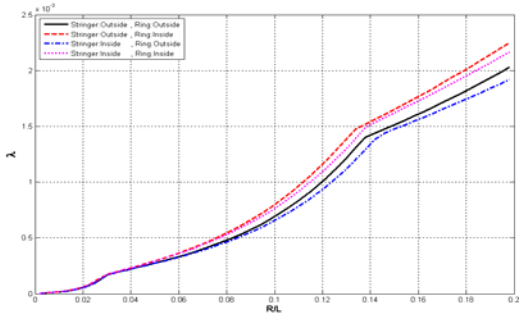

Fig. 12
Lateral pressure buckling parameter λ, for stringers and rings stiffened cylindrical shell ($R / L\langle 0.2$).

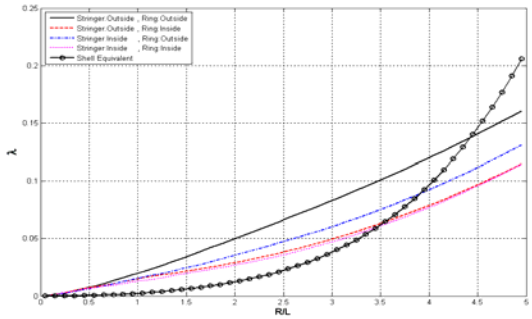

Fig. 13
Hydrostatic pressure buckling parameter λ, for stringers and rings stiffened cylindrical shell ($R / L\langle 5$).

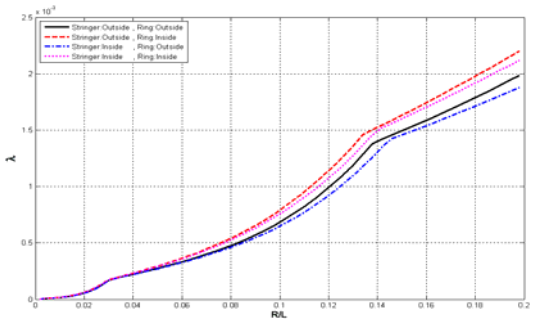

Fig. 14
Hydrostatic pressure buckling parameter λ, for stringers and rings stiffened cylindrical shell ($R / L\langle 0.2$).

The buckling load parameter curve of unstiffened shell of Fig. 13 shows that, with high *R*/*L* ratio, the stability of unstiffened shell is more than the stability of stiffened cylindrical shell with stringers and rings.

5 CONCLUDING REMARKS

According to our numerical results and comparisons, the following concluding remarks are itemized:
- In stability of stiffened cylindrical shells under axial pressure loading, the cylinders reinforced with outer rings are more stable than the inner one. In this case, the stability is independent of the length of the cylinders. The critical buckling load decreases with increasing eccentricity of the reinforced inner rings. For the outer ring cases, however, the eccentricity has almost no effect on the critical buckling load.
- In cylindrical shells stiffened with stringers, the stability of cylinders with outer stringers is higher than the inner one. Also, the critical buckling load increases with increasing the eccentricity of the stringers.
- The stability of cylinders stiffened by stringers under axial loading is much higher than the hydrostatic lateral loadings
- In general, stability of the stiffened cylindrical shells under hydrostatic lateral loading, the ring stiffeners are more stable than the stringers one. Also, the stability behavior of the stiffened long cylinders under hydrostatic lateral loading is very close to each other.

APPENDIX A

The shell partitioned stiffness matrix $[K]^c$ is summarized as

$$[K]^c = \begin{bmatrix} [K_{pp}] & [K_{pq}] & [K_{pr}] \\ [K_{pq}]^T & [K_{qq}] & [K_{qr}] \\ [K_{pr}]^T & [K_{qr}]^T & [K_{rr}] \end{bmatrix} \tag{A.1}$$

The elements of the shell stiffness submatrices are given by

$$\left[K_{pp}\right]_{ij} = 2\xi^2\alpha^2 \int_0^1 \frac{d\overline{u}_i}{d\overline{x}} \frac{d\overline{u}_j}{d\overline{x}} \mathrm{d}\overline{x} \; + \; \xi^2 n^2 \left(1-\nu\right)\left(1+\frac{\xi^2}{48}\right)\int_0^1 \overline{u}_i \overline{u}_j \; \mathrm{d}\overline{x} \tag{A.2}$$

$$\left[K_{pq}\right]_{ij} = \xi^2\alpha n\left[(1-\nu)\left(1-\frac{\xi^2}{16}\right)\int_0^1 \overline{u}_i \frac{\mathrm{d}\overline{v}_j}{\mathrm{d}\overline{x}} \mathrm{d}\overline{x} \; - \; 2\nu \int_0^1 \frac{\mathrm{d}\overline{u}_i}{\mathrm{d}\overline{x}} \overline{v}_j \mathrm{d}\overline{x}\right] \tag{A.3}$$

$$\left[K_{pr}\right]_{ij} = -\alpha n^2 (1-\nu)\frac{\xi^4}{12}\int_0^1 \overline{u}_i \frac{\mathrm{d}\overline{w}_j}{\mathrm{d}\overline{x}} \mathrm{d}\overline{x} \; - \; 2\xi^2\alpha\nu \int_0^1 \frac{\mathrm{d}\overline{u}_i}{\mathrm{d}\overline{x}} \overline{w}_j \; \mathrm{d}\overline{x} \tag{A.4}$$

$$\left[K_{qq}\right]_{ij} = 2\xi^2 n^2 \int_0^1 \overline{v}_i \overline{v}_j \; \mathrm{d}\overline{x} \; + \; \xi^2\alpha^2 (1-\nu)\left(1+\frac{3\xi^2}{16}\right)\int_0^1 \frac{\mathrm{d}\overline{v}_i}{\mathrm{d}\overline{x}} \frac{\mathrm{d}\overline{v}_j}{\mathrm{d}\overline{x}} \mathrm{d}\overline{x} \tag{A.5}$$

$$\left[K_{qr}\right]_{ij} = 2\xi n \int_0^1 \overline{v}_i \overline{w}_j \mathrm{d}\overline{x} \; + \; \alpha^2 n \frac{\xi^3}{4}(1-\nu)\int_0^1 \frac{\mathrm{d}\overline{v}_i}{\mathrm{d}\overline{x}} \frac{\mathrm{d}\overline{w}_j}{\mathrm{d}\overline{x}} \mathrm{d}\overline{x} \tag{A.6}$$

$$\begin{aligned}\left[K_{rr}\right]_{ij} = &\left(2+\frac{\xi^2}{6}(1-n^2)^2\right)\int_0^1 \overline{w}_i \overline{w}_j \mathrm{d}\overline{x} + \alpha^4 \frac{\xi^2}{6}\int_0^1 \frac{\mathrm{d}^2\overline{w}_i}{\mathrm{d}\overline{x}^2} \frac{\mathrm{d}^2\overline{w}_j}{\mathrm{d}\overline{x}^2} \mathrm{d}\overline{x} \\ &+\frac{\xi^2}{6}\nu\alpha^2(1-n^2)\left(\int_0^1 \frac{\mathrm{d}^2\overline{w}_i}{\mathrm{d}\overline{x}^2}\overline{w}_j \mathrm{d}\overline{x} + \int_0^1 \overline{w}_i \frac{\mathrm{d}^2\overline{w}_j}{\mathrm{d}\overline{x}^2}\mathrm{d}\overline{x}\right) \\ &+\frac{\xi^2}{3}\alpha^2 n^2 (1-\nu)\int_0^1 \frac{\mathrm{d}\overline{w}_i}{\mathrm{d}\overline{x}} \frac{\mathrm{d}\overline{w}_j}{\mathrm{d}\overline{x}} \mathrm{d}\overline{x}\end{aligned} \tag{A.7}$$

The stringer partitioned stiffness matrix $\left[K\right]^s_{\theta=\theta_s}$ is summarized as

$$\left[K\right]^s_{\theta=\theta_s} = \frac{(1-\nu^2)}{\pi} E_s \begin{bmatrix} \left[K_{spp}\right] & \left[K_{spq}\right] & \left[K_{spr}\right] \\ \left[K_{spq}\right]^T & \left[K_{sqq}\right] & \left[K_{sqr}\right] \\ \left[K_{spr}\right]^T & \left[K_{sqr}\right]^T & \left[K_{srr}\right] \end{bmatrix}_{\theta=\theta_s} \tag{A.8}$$

The elements of the stringer stiffness submatrices are given by

$$\left[K_{spp}\right]_{ij} = 2\xi^3 \hat{\alpha}^2 \overline{\mathrm{A}}_{\mathrm{s}} \sin^2 n\theta \int_0^1 \frac{\mathrm{d}\overline{u}_i}{\mathrm{d}\overline{x}} \frac{\mathrm{d}\overline{u}_j}{\mathrm{d}\overline{x}} \; \mathrm{d}\overline{x} \tag{A.9}$$

$$\left[K_{spq}\right]_{ij} = -2\overline{c}_s h\alpha^4 \xi^3 \overline{\mathrm{A}}_{\mathrm{s}} \sin \mathrm{n}\theta \cos \mathrm{n}\theta \int_0^1 \frac{\mathrm{d}\overline{u}_i}{\mathrm{d}\overline{x}} \frac{\mathrm{d}^2\overline{v}_j}{\mathrm{d}\overline{x}^2} \; \mathrm{d}\overline{x} \tag{A.10}$$

$$\left[K_{spr}\right]_{ij} = 2\overline{e}_s h\xi^2 \hat{\alpha}^2 \overline{\mathrm{A}}_{\mathrm{s}} \sin^2 n\theta \int_0^1 \frac{\mathrm{d}\overline{u}_i}{\mathrm{d}\overline{x}} \frac{\mathrm{d}^2\overline{w}_j}{\mathrm{d}\overline{x}^2} \; \mathrm{d}\overline{x} \tag{A.11}$$

$$\left[K_{sqq}\right]_{ij} = 2(\overline{c}_s^2 h^2 \alpha^4 \xi^3 \overline{\mathrm{A}}_{\mathrm{s}} \cos^2 n\theta + \hat{\alpha}^2 \xi^2 \mathrm{h}^2 \overline{\mathrm{I}}_{\mathrm{zs}} \cos^2 \mathrm{n}\theta)\left(\int_0^1 \frac{\mathrm{d}^2\overline{v}_i}{\mathrm{d}\overline{x}^2} \frac{\mathrm{d}^2\overline{v}_j}{\mathrm{d}\overline{x}^2} \; \mathrm{d}\overline{x}\right) \tag{A.12}$$

$$\begin{aligned}\left[K_{sqr}\right]_{ij} = &\left[-2\overline{e}_s \overline{c}_s h^2 \xi^2 \alpha^4 \overline{\mathrm{A}}_{\mathrm{s}} \sin \mathrm{n}\theta \cos n\theta + 2e_s n\hat{\alpha}^2 \xi^2 \mathrm{h}^2 \overline{\mathrm{I}}_{\mathrm{zs}} \cos^2 \mathrm{n}\theta\right. \\ &\left. + 2\hat{\alpha}^2 \xi \mathrm{h}^2 \overline{\mathrm{I}}_{\mathrm{yzs}} \cos \mathrm{n}\theta(\sin \mathrm{n}\theta + \overline{\mathrm{c}}_{\mathrm{s}} \mathrm{n}\xi \cos \mathrm{n}\theta)\right] \times \left(\int_0^1 \frac{\mathrm{d}^2\overline{v}_i}{\mathrm{d}\overline{x}^2} \frac{\mathrm{d}^2\overline{w}_j}{\mathrm{d}\overline{x}^2} \; \mathrm{d}\overline{x}\right)\end{aligned} \tag{A.13}$$

$$\left[K_{srr}\right]_{ij}=\frac{\overline{J}_s\alpha^2\xi^2n^2}{(1+\nu)}cos^2n\theta\int_0^1\frac{\mathrm{d}\overline{w}_i}{\mathrm{d}\overline{x}}\frac{\mathrm{d}\overline{w}_j}{\mathrm{d}\overline{x}}\,\mathrm{d}\overline{x}+2\Big\{\xi\alpha^2\overline{e}_s^2h^2\overline{\mathrm{A}}_s\sin^2n\theta+\overline{e}_s^2n^2\overline{\mathrm{I}}_{zs}\mathrm{h}^2\alpha^2\xi^2\cos^2n\theta$$
$$+\overline{I}_{ys}h^2\alpha^2\left[\sin n\theta+\overline{c}_sn\xi\,\cos n\theta\right]^2+2\overline{e}_sn\alpha^2\xi h^2\overline{I}_{yzs}\cos n\theta\,(\sin n\theta+\overline{\mathrm{c}}_sn\xi\,\cos n\theta)\Big\}\int_0^1\frac{\mathrm{d}^2\overline{w}_i}{\mathrm{d}\overline{x}^2}\frac{\mathrm{d}^2\overline{w}_j}{\mathrm{d}\overline{x}^2}\,\mathrm{d} \tag{A.14}$$

The ring partitioned stiffness matrix $\left[K\right]_{x=L_k}^k$ is summarized as

$$\left[K\right]_{x=L_k}^k=\frac{1-\nu^2}{(1+\xi\overline{e}_k)^3}\overline{E}_k\alpha\xi^2\begin{bmatrix}\left[K_{kpp}\right] & 0 & \left[K_{kpr}\right]\\ 0 & \left[K_{kqq}\right] & \left[K_{kqr}\right]\\ \left[K_{kpr}\right]^T & \left[K_{kqr}\right]^T & \left[K_{krr}\right]\end{bmatrix}_{x=L_k} \tag{A.15}$$

The elements of the ring stiffness submatrices are given by

$$\left[K_{kpp}\right]_{ij}=2n^2\xi^2\left(\overline{I}_{zk}n^2+\frac{\overline{J}_k}{2\left(1+\nu_k\right)}\right)\overline{u}_{i(L_k)}\overline{u}_{j(L_k)} \tag{A.16}$$

$$\left[K_{kpr}\right]_{ij}=-2n^2\xi\left(\overline{I}_{zk}\alpha(1+\xi\overline{e}_k-n^2\xi\overline{e}_k)+\frac{\alpha\overline{J}_k}{2(1+\nu_k)}\right)\left(\overline{u}_{i(L_k)}\frac{d\overline{w}_{j(L_k)}}{d\overline{x}}\right) \tag{A.17}$$

$$\left[K_{kqq}\right]_{ij}=2n^2\xi\overline{A}_k(1+\xi\overline{e}_k)^4\overline{v}_{i(L_k)}\overline{v}_{j(L_k)} \tag{A.18}$$

$$\left[K_{kqr}\right]_{ij}=2n\overline{A}_k(1+\xi\overline{e}_kn^2)(1+\xi\overline{e}_k)^3\overline{v}_{i(L_k)}\overline{w}_{j(L_k)} \tag{A.19}$$

$$\left[K_{krr}\right]_{ij}=2\alpha^2\left(\overline{I}_{zk}(1+\xi\overline{e}_k-n^2\xi\overline{e}_k)^2+\frac{n^2\overline{J}_k}{2(1+\nu_k)}\right)\frac{d\overline{w}_{i(L_k)}}{d\overline{x}}\frac{d\overline{w}_{j(L_k)}}{d\overline{x}}$$
$$+2\left(\overline{I}_{xk}(1-n^2)^2+\frac{\overline{A}_k}{\xi}(1+\xi\overline{e}_kn^2)^2(1+\xi\overline{e}_k)^2\right)\overline{w}_{i(L_k)}\overline{w}_{j(L_k)} \tag{A.20}$$

and

$$\left[G\right]=\begin{bmatrix}0 & 0 & 0\\ 0 & 0 & 0\\ 0 & 0 & \left[G_{rr}\right]\end{bmatrix} \tag{A.21}$$

where

$$\left[G_{rr}\right]_{ij}=2\left(1-n^2\right)\int_0^1\psi\overline{w}_i\overline{w}_j\mathrm{d}\overline{x}-\frac{\beta}{2}\alpha^2\int_0^1\frac{d\overline{w}_i}{d\overline{x}}\frac{d\overline{w}_j}{d\overline{x}}\mathrm{d}\overline{x} \tag{A.22}$$

where $i, j = 1,\ 2,\ 3.$

REFERENCES

[1] Singer J., Baruch M., 1963, Effect of eccentricity of stiffeners on the general instability of stiffened cylindrical shells under hydrostatic pressure, *International Journal of Mechanical Sciences* **5**: 23-27.
[2] Ghorbanpour A., Golabi S., Loghman A., Daneshi H., 2007, Investigating elastic stability of cylindrical shell with an elastic core under axial compression by energy method, *Journal of Mechanical Science and Technology* **21**(7): 983-996.
[3] Ojalvo I.U., Newman M., 1967, Natural vibrations of a stiffened pressurized cylinder with an attached mass, *AIAA. Journal* **5**: 1139-1146.
[4] Eslami M.R., Ziaii A.R., Ghorbanpour A., 1996, Thermoelastic buckling of thin cylindrical shell based on improved stability equations, *Journal of Thermal Stresses* **19**: 299-315.
[5] Singer J., Baruch M., Harari O., 1967, The stability of eccentrically stiffened cylindrical shells under axial compression, *International Journal of Solids and Structures* **3**: 445-470.
[6] Hubner A., Albiez M., Kohler D., Saal H., 2007, Buckling of long steel cylindrical shells subjected to external pressure, *Thin-Walled Structures* **45**: 1-7.
[7] Buermann P., Rolfes R., Tessmer J., Schagerlet M., 2006, A semi- analytical model for local post-buckling analysis of stringer- and frame-stiffened cylindrical panels, *Thin-Walled Structures* **44**: 102-114.
[8] Ding H., 2003, Strength and stability of double cylindrical shell structure subjected to hydrostatic external pressure—II: stability, *Marine Structures* **16**: 397-415.
[9] Andrianova V.M., Verbonolb J., Awrejcewiczc I.V., 2006, Buckling analysis of discretely stringer-stiffened cylindrical shells, *International Journal of Mechanical Sciences* **48**: 1505-1515.
[10] Timoshenko S.P., Gere J.M., 1985, *Theory of Elastic Stability,* Mc-Graw Hill, NewYork.
[11] Galletly G.D, 1955, On the in-vacuo vibrations of simply supported ring-stiffened cylindrical shells, *ASME Proceedings of 2nd U.S. National Congress of Applied Mechanics*: 225-231.
[12] Wang Y.G., Zeng G.W., 1983, Calculation of critical pressure of ring stiffened cylindrical shells through function minimization, *China Ship Building* **4**: 29-38.
[13] Bushnell D., 1985, *Computerized Buckling Analysis of Shells*, Martinus Nijhoff Publishers, Lancaster.